Magn. Reson. Discuss.,
https://doi.org/10.5194/mr-2020-26-AC2, 2020

Open Access MAGNETIC RESONANCE Discussions

Interactive comment on "Phosphoserine for the generation of lanthanide binding sites on proteins for paramagnetic NMR" *by* Sreelakshmi Mekkattu Tharayil et al.

Sreelakshmi Mekkattu Tharayil et al.

gottfried.otting@anu.edu.au

Received and published: 30 November 2020

We are grateful for the insightful comments and identifying errors.

Comment 1: The authors should comment that the axial anisotropies of the proposed tag attached to ubiquitin with a single phosphoserine mutation are significantly smaller than those of other previously proposed rigid tags (more than a factor 2 for Tb probes, more than a factor 5 for Tm), and should discuss the origin of this difference.

Response: The same point was picked up by Marcellus Ubbink and our response is copied here.

Indeed, the difference in DeltaChi tensors obtained with Tm3+ and Tb3+ was larger than expected for the single-Sep mutants (but not for the GB1 mutant A24Sep/K28Sep). We observed previously that the ratio between the axial tensor components of these two ions can vary between different tags and even for the same tag at different sites of a protein (C.-T. Loh, B. Graham, E. H. Abdelkader, K. L. Tuck, G. Otting (2015) Generation of pseudocontact shifts in proteins with lanthanides using small "clickable" nitrilotriacetic acid and iminodiacetic acid tags Chem. Eur. J. 21, 5084-5092). These differences are not an artifact of fitting the tensors for Tm3+ and Tb3+ independently, as the fits yielded very similar coordinates for both metal ions. We do not understand the origin of these effects. It would help, if the effect of the ligand field could be predicted by quantum-mechanical calculations, but we were told by experts in the field that this is prohibitively difficult for lanthanide ions.

In the revised version, we propose to add the following paragraph in line 371: "The DeltaChi tensors obtained with Tm3+ instead of Tb3+ ions were unexpectedly low for the single-Sep mutants, but not for the GB1 mutant A24Sep/K28Sep. We observed previously that the ratio between the DeltaChi_axial components of these two ions can vary between different tags and even for the same tag at different sites of a protein (Loh et al., 2015). These differences are not an artifact of fitting the tensors for Tm3+ and Tb3+ independently, as, with the exception of ubiquitin E18Sep, the fits converged to very similar metal positions (Tables 1 and 2). We do not understand the origin of different magnitudes of Chi-tensor anisotropies for Tm3+ and Tb3+ ions. In addition, much larger DeltaChi tensors have been reported for sterically rigid cyclen tags (Joss and Häussinger, 2019), suggesting that a rigid ligand field promotes large DeltaChi tensors."

Comment 2: The tensor for the GB1 K10D/T11Sep(Tb3+) should be reported with an axial component of -33.7 and a rhombic component of 14.7 to fulfill the axis labeling convention providing a rhombic component up to 2/3 of the axial component in absolute value. If the authors prefer to report the tensor as in Table 1, they should at least explain why. In any case, the tensor anisotropy is surprisingly large considering that the measured pcs span a range smaller than that measured for ubiquitin, and surprisingly rather rhombic. In the double phosphoserine K10Sep/T11Sep (Tb3+) mutant, the measured values of the pcs span a range which is roughly double, but the tensor is less than half with respect to that of K10D/T11Sep(Tb3+). Please, double check that no mix-up of data has occurred.

Response: Thank you for alerting us to this typo. The correct numbers for DeltaChi_axial and DeltaChi_rhombic are 7.3 and 1.6, respectively.

Comment 3: Can you comment on the reason of the different sign of the tensor axial components between K10Sep/T11Sep(Tb3+) and A24Sep/K28Sep(Tb3+)? On the other hand, the sign of the axial components of Tb and Tm are usually opposite. Why are they the same in A24Sep/K28Sep.

Response: We do not understand the reason for the sign change in the tensor for Tb3+ between the K10Sep/T11Sep and A24Sep/K28Sep mutants. We double-checked and couldn't find an error. The signs were indeed wrong for the Tm3+ tensor associated with GB1 A24Sep/K28Sep(Tm3+): the correct values for the axial and rhombic components are -15.5 and -2.5, respectively.

In the revised version, we will display the isosurfaces also for Tm3+ in Figures 2, 3 and 4 to illustrate the degree of orthogonality of the tensors between Tm3+ and Tb3+ (revised Figures attached).

Comment 4: Minor points: Pag.2, line 1: "As lanthanide ions display particularly large. . ." not all lanthanoids, only some of them! Pag. 2, line 2: "While paramagnetic lanthanide ions generate paramagnetic relaxation enhancements (PRE) in the protein irrespective of metal mobility" This sentence may be read that PREs do not depend on mobility, which is slightly inaccurate, because internal mobility changes the correlation time of dipole-dipole relaxation (see Fragai et al. Coord. Chem. Rev. 2013, 257, 2652 for a thorough discussion). Please, clarify this point. Caption to Fig. 3: please indicate

all panel letters.

Response: In the revised version, we propose the following changes. Page 2, line 1: "As many lanthanide ions display particularly large. . ." Page 2, paragraph 2: "Paramagnetic lanthanide ions always generate paramagnetic relaxation enhancements (PRE) in the protein, which vary relatively little with minor movements of the metal ion. In contrast, PCSs can decrease dramatically if the lanthanide complex reorientates relative to the protein."

Interactive comment on Magn. Reson. Discuss., https://doi.org/10.5194/mr-2020-26, 2020.

Table 1. $\Delta\chi$-tensor parameters of the ubiquitin mutants E18Sep, E16Q/E18Sep and T22Sep/N25D/K29Q and the GB1 mutant K10D/T11Sep complexed with Tb^{3+} and Tm^{3+} ions.[a]

Protein	N[b]	$\Delta\chi_{ax}$[c] (10^{-32} m^3)	$\Delta\chi_{rh}$[c] (10^{-32} m^3)	x (Å)	y (Å)	z (Å)	α (°)	β (°)	γ (°)	Q[d]
ubiquitin E18Sep (Tb^{3+})	20	17.1 (0.6)	2.8 (0.3)	10.095	-1.846	-11.711	170	138	50	0.03
ubiquitin E18Sep (Tm^{3+})	27	-2.7 (0.1)	-1.0 (0.1)	9.463	-0.674	-12.207	168	129	49	0.03
ubiquitin E16Q/E18Sep (Tb^{3+})	27	15.9 (0.6)	3.4 (0.8)	9.695	-1.754	-11.833	162	135	37	0.04
ubiquitin E16Q/E18Sep (Tm^{3+})	28	-4.5 (0.1)	-2.1 (0.1)	9.441	-1.902	-11.918	164	131	59	0.03
GB1 K10D/T11Sep (Tb^{3+})	26	7.3 (0.1)	1.6 (0.1)	3.513	14.367	0.093	35	116	174	0.01
ubi. T22Sep/N25D/K29Q (Tb^{3+})	20	3.5 (0.1)	1.3 (0.1)	5.505	1.144	-8.867	150	104	9	0.03

[a] The $\Delta\chi$-tensor fits used PCSs measured with Tb^{3+} and Tm^{3+}, using Y^{3+} as the diamagnetic reference. The metal coordinates and tensor parameters for the ubiquitin and GB1 mutants are reported relative to the NMR ensemble structure of ubiquitin (PDB ID: 2KOX; Fenwick et al., 2011) and the crystal structure of GB1 (PDB ID: 1PGA; Gallagher et al., 1994), respectively.

[b] N: number of PCSs used in the fit.

[c] Uncertainties (in brackets) were determined from fits obtained by randomly omitting 10 % of the PCS data.

[d] The quality factor was calculated as the root-mean-square deviation between experimental and back-calculated PCSs divided by the root-mean-square of the experimental PCSs.

Fig. 1. revised Table 1

Table 2. $\Delta\chi$-tensor parameters of the GB1 mutants K10Sep/T11Sep and A24Sep/K28Sep.[a]

Mutant	N	$\Delta\chi_{ax}$ (10^{-32} m^3)	$\Delta\chi_{rh}$ (10^{-32} m^3)	x (Å)	y (Å)	z (Å)	α (°)	β (°)	γ (°)	Q
K10Sep/T11Sep (Tb^{3+})	31	-14.5 (0.1)	-3.2 (0.1)	27.455	13.449	12.675	88	13	155	0.01
A24Sep/K28Sep (Tb^{3+})	34	34.7 (0.6)	5.3 (0.1)	17.628	34.049	21.869	178	46	69	0.02
A24Sep/K28Sep (Tm^{3+})	31	-15.5 (0.4)	-2.5 (0.1)	17.666	34.141	21.937	178	46	47	0.03

[a] The $\Delta\chi$-tensor fits used the crystal structure 1PGA (Gallagher et al., 1994) and the PCSs measured with Tb^{3+} (or Tm^{3+}) and Y^{3+}. See footnotes b-d of Table 1 for further details.

Fig. 2. revised Table 2

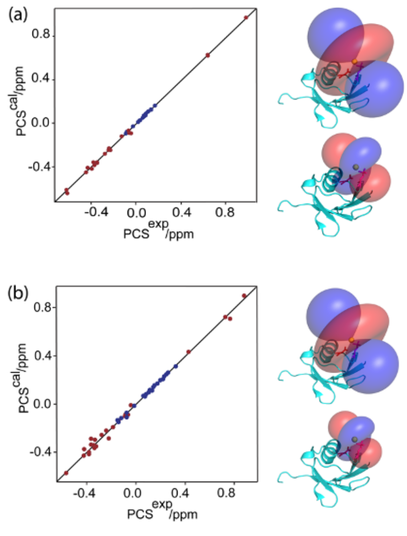

9

Figure 2. Correlation between back-calculated and experimental PCSs, and lanthanide locations on the ubiquitin mutants (a) E18Sep and (b) E16Q/E18Sep. Left panel: PCS data obtained with Tb^{3+} and Tm^{3+} plotted in red and blue, respectively. Right panel: Blue and red PCS isosurfaces plotted on the protein structure and indicating PCSs of +/-1 ppm, respectively. The isosurfaces illustrate the $\Delta\chi$ tensors obtained with Tb^{3+} (upper structure) and Tm^{3+} (lower structure). The side chains of E16 and the phosphoserine residue in position 18 are shown in a stick representation.

Fig. 3. revised Figure 2

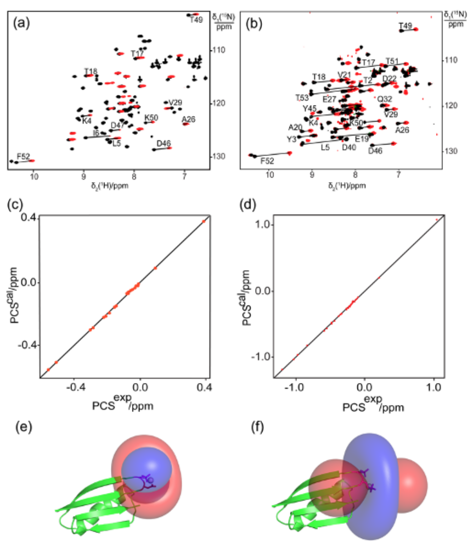

11

Figure 3. Close agreement between experimental and back-calculated PCSs of amide protons in the protein GB1 obtained with lanthanide binding sites generated with one or two phosphoserine residues. (a) and (b) Superimposition of [^{15}N,^{1}H]-HSQC spectra of 0.3 mM solutions of GB1 K10D/T11Sep and GB1 K10Sep/T11Sep, respectively. The spectra were recorded in the presence of Tb^{3+} (red) or Y^{3+} (black). Lines connect cross-peaks belonging to the same residue in the paramagnetic and diamagnetic samples. (c) and (d) Correlation between back-calculated and experimental PCSs for GB1 K10D/T11Sep and GB1 K10Sep/T11Sep, respectively. (e) and (f) Location of the Tb^{3+} ion on the GB1 mutants K10D/T11Sep and K10Sep/T11Sep, respectively, and PCS isosurfaces plotted on the structure of GB1. Blue and red isosurfaces indicate PCSs of +/-1 ppm, respectively.

Fig. 4. revised Figure 3

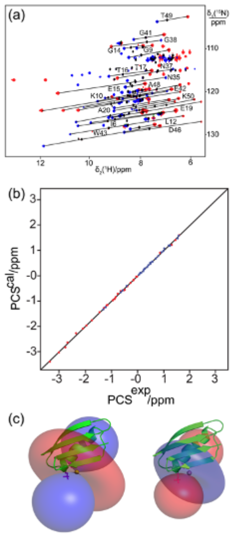

Figure 4. The double-phosphoserine mutant GB1 A24Sep/K28Sep generates high-quality PCSs. (a) Superimposition of [^{15}N,^1H]-HSQC spectra of 0.3 mM solutions of GB1 A24Sep/K28Sep in the presence of one equivalent of Tb^{3+} (red cross-

14

peaks), Tm^{3+}(blue cross-peaks) or Y^{3+} (black cross-peaks). Lines were drawn to connect selected corresponding cross-peaks observed with diamagnetic and paramagnetic metal ions. (b) Correlation between back-calculated and experimental PCSs. (c) Blue and red isosurfaces indicating PCSs of +/-1 ppm, respectively, as determined by the $\Delta\chi$-tensors of Tb^{3+} (left) and Tm^{3+} (right). The side chains of Sep residues modelled at positions 24 and 28 are highlighted by a stick representation.

Fig. 5. revised Figure 4